The intermediate neutron-capture process in stars, and its abundance signatures in presolar grains

Marco Pignatari

University of Basel, Switzerland

Ambizione grant - SNSF

www.nugridstars.org

F. Herwig, M. Bertolli, P. Woodward, S. Jones, R. Hirschi

E. Zinner, P. Hoppe, M. Jadhav, W. Fujiya, N. Liu

What is the Origin of the Elements?

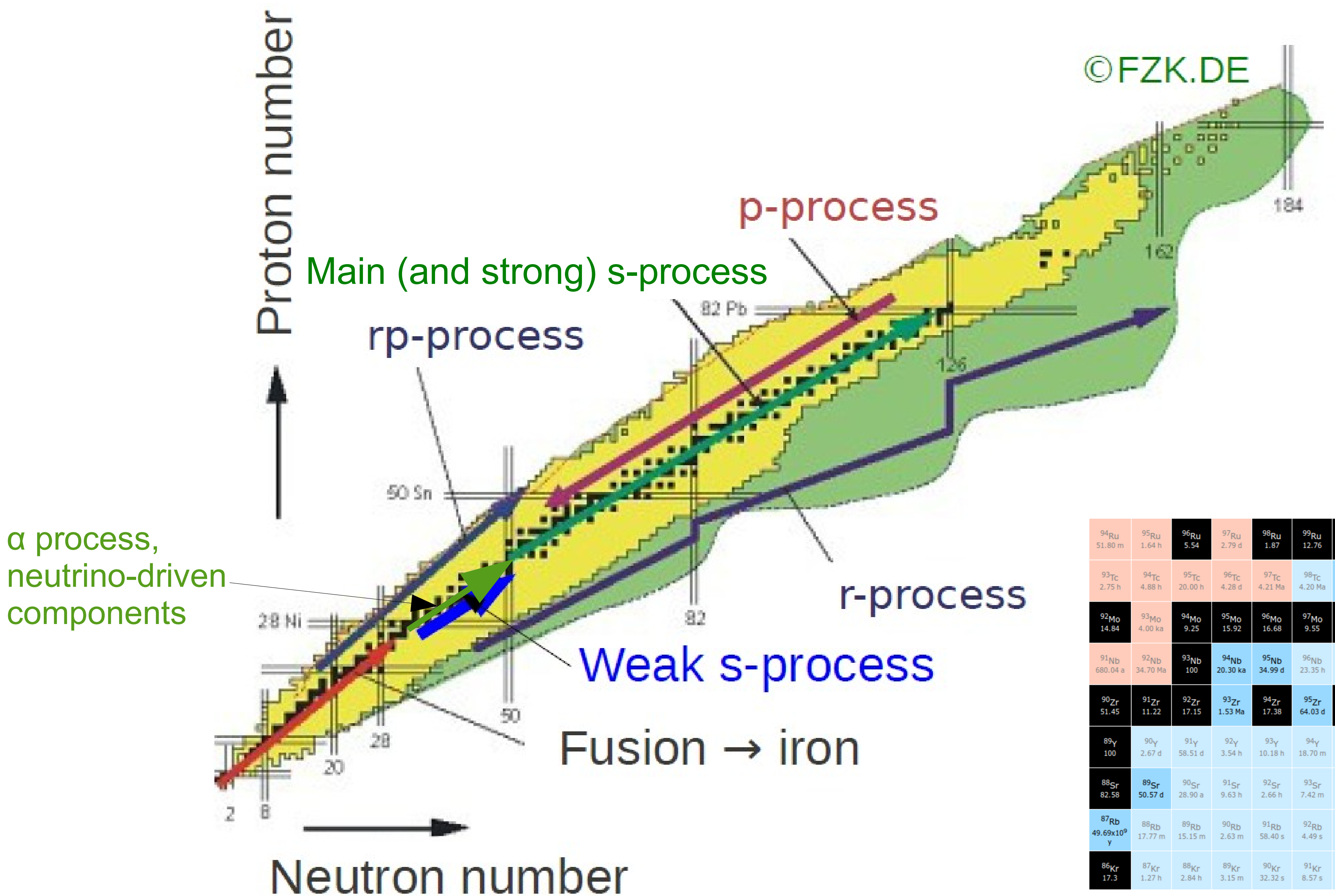

^{94}Ru 51.80 m	^{95}Ru 1.64 h	^{96}Ru 5.54	^{97}Ru 2.79 d	^{98}Ru 1.87	^{99}Ru 12.76	^{100}Ru 12.6	^{101}Ru 17.06	^{102}Ru 31.55
^{93}Tc 2.75 h	^{94}Tc 4.88 h	^{95}Tc 20.00 h	^{96}Tc 4.28 d	^{97}Tc 4.21 Ma	^{98}Tc 4.20 Ma	^{99}Tc 211.11 ka	^{100}Tc 15.80 s	^{101}Tc 14.22 m
^{92}Mo 14.84	^{93}Mo 4.00 ka	^{94}Mo 9.25	^{95}Mo 15.92	^{96}Mo 16.68	^{97}Mo 9.55	^{98}Mo 24.13	^{99}Mo 2.75 d	^{100}Mo 9.63
^{91}Nb 680.04 a	^{92}Nb 34.70 Ma	^{93}Nb 100	^{94}Nb 20.30 ka	^{95}Nb 34.99 d	^{96}Nb 23.35 h	^{97}Nb 1.20 h	^{98}Nb 2.86 s	^{99}Nb 15.00 s
^{90}Zr 51.45	^{91}Zr 11.22	^{92}Zr 17.15	^{93}Zr 1.53 Ma	^{94}Zr 17.38	^{95}Zr 64.03 d	^{96}Zr 2.8	^{97}Zr 16.74 h	^{98}Zr 30.70 s
^{89}Y 100	^{90}Y 2.67 d	^{91}Y 58.51 d	^{92}Y 3.54 h	^{93}Y 10.18 h	^{94}Y 18.70 m	^{95}Y 10.30 m	^{96}Y 5.34 s	^{97}Y 3.75 s
^{88}Sr 82.58	^{89}Sr 50.57 d	^{90}Sr 28.90 a	^{91}Sr 9.63 h	^{92}Sr 2.66 h	^{93}Sr 7.42 m	^{94}Sr 1.25 m	^{95}Sr 23.90 s	^{96}Sr 1.07 s
^{87}Rb 49.69×10^{9} y	^{88}Rb 17.77 m	^{89}Rb 15.15 m	^{90}Rb 2.63 m	^{91}Rb 58.40 s	^{92}Rb 4.49 s	^{93}Rb 5.84 s	^{94}Rb 2.70 s	^{95}Rb 377.00 ms
^{86}Kr 17.3	^{87}Kr 1.27 h	^{88}Kr 2.84 h	^{89}Kr 3.15 m	^{90}Kr 32.32 s	^{91}Kr 8.57 s	^{92}Kr 1.84 s	^{93}Kr 1.29 s	^{94}Kr 212.00 ms

Sneden, Cowan & Gallino 2008

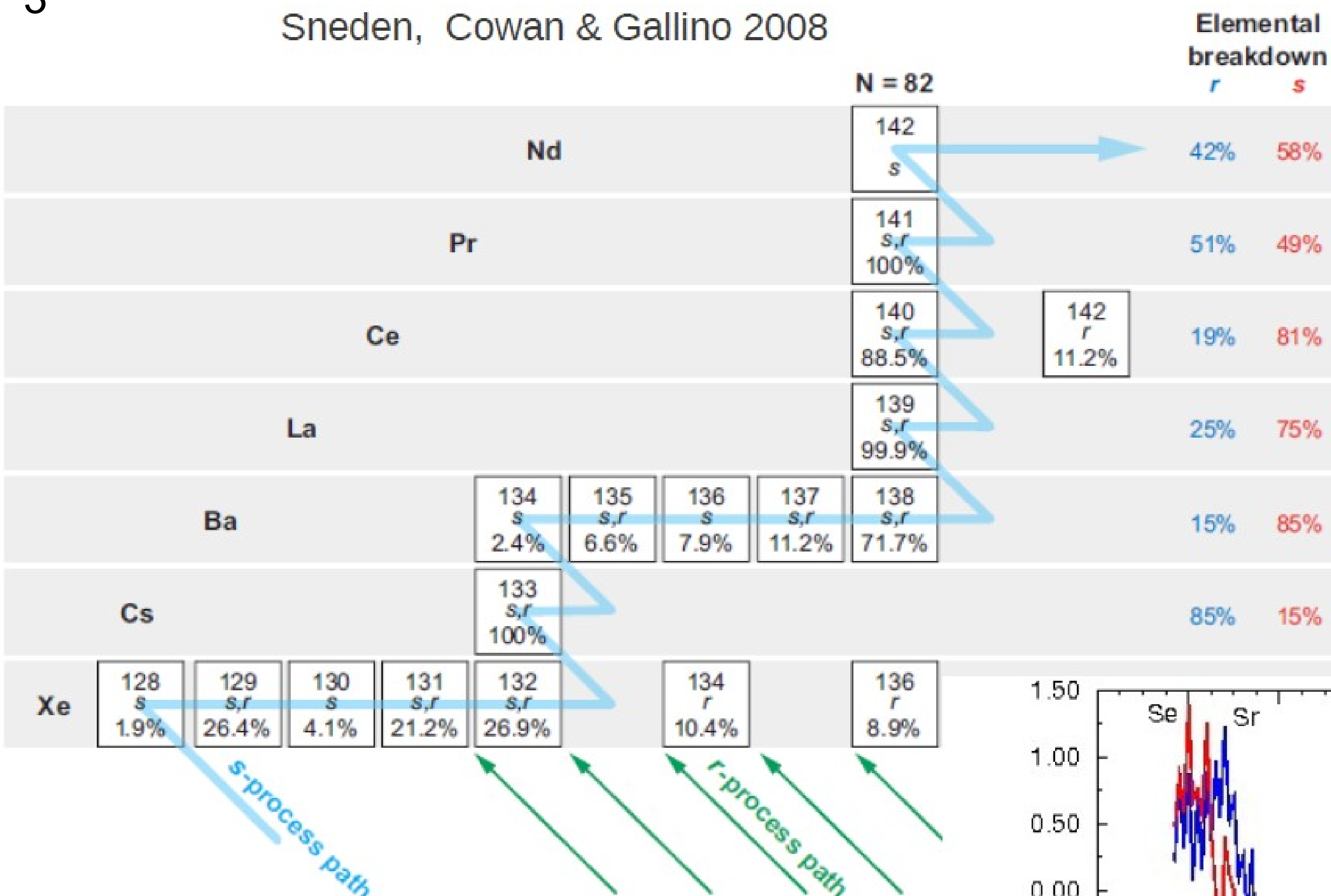

S-process path along the valley of stability in stars, starting from Fe seeds

$10^6 - (10^{12})$ n cm^{-3}

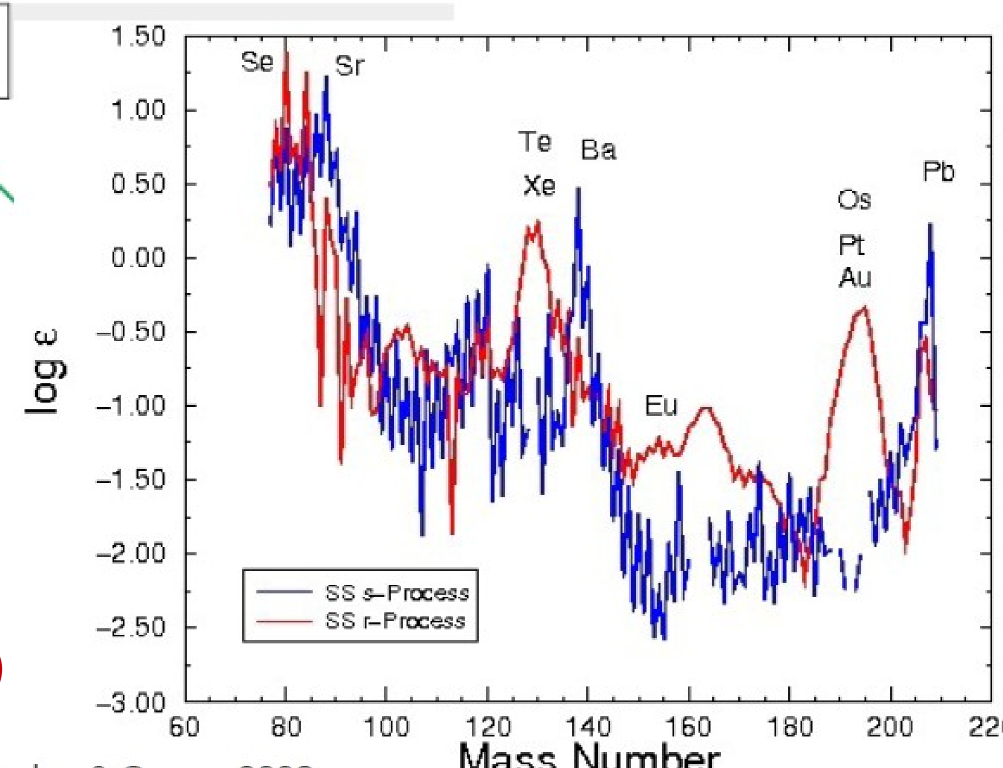

Sneden & Cowan 2003

S-process signature identifiable in the solar system distribution

weak, main and strong s-process components (GCE included)

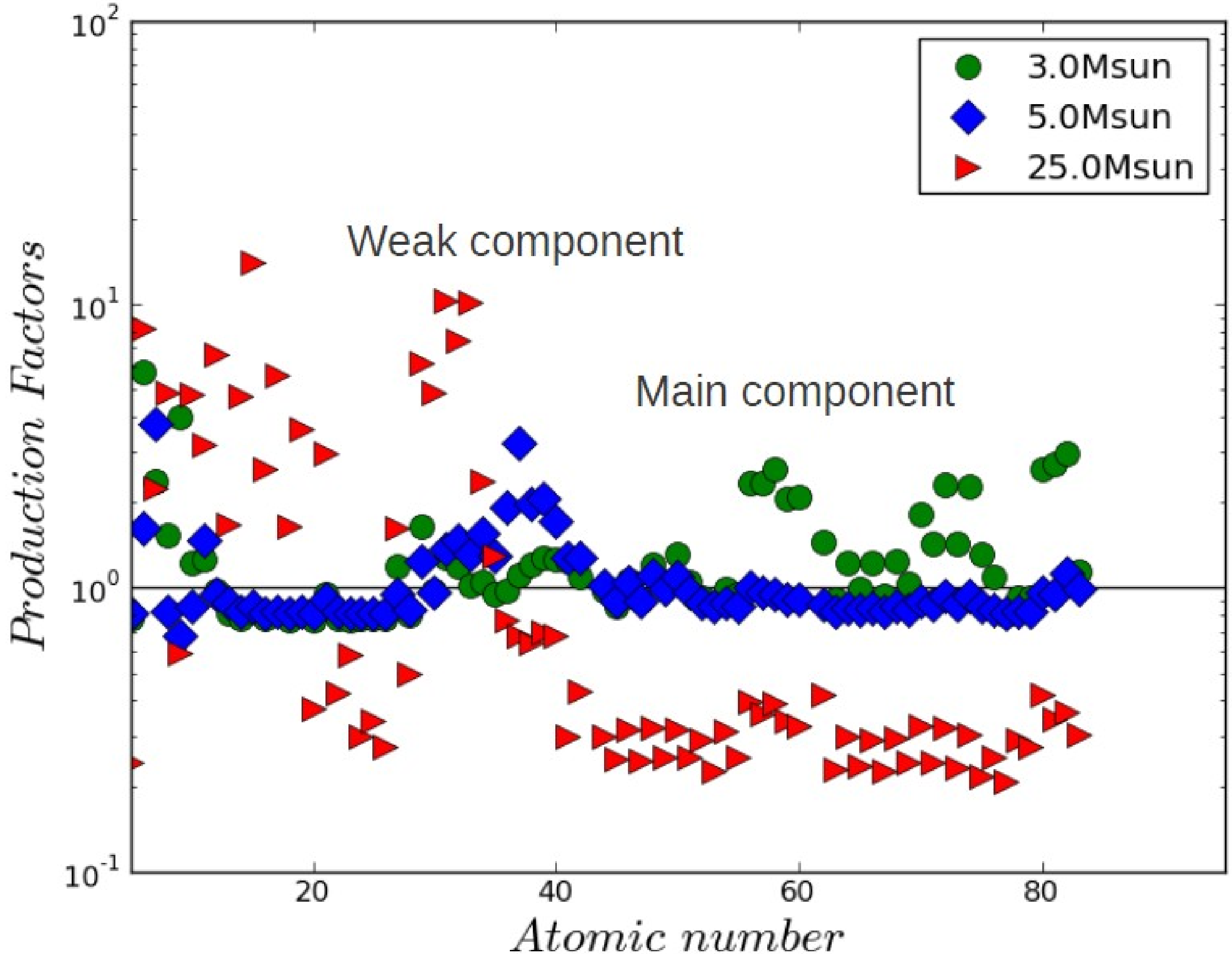

Elemental production factors for a low mass AGB star, a massive AGB stars, and a massive star (Z=0.01).

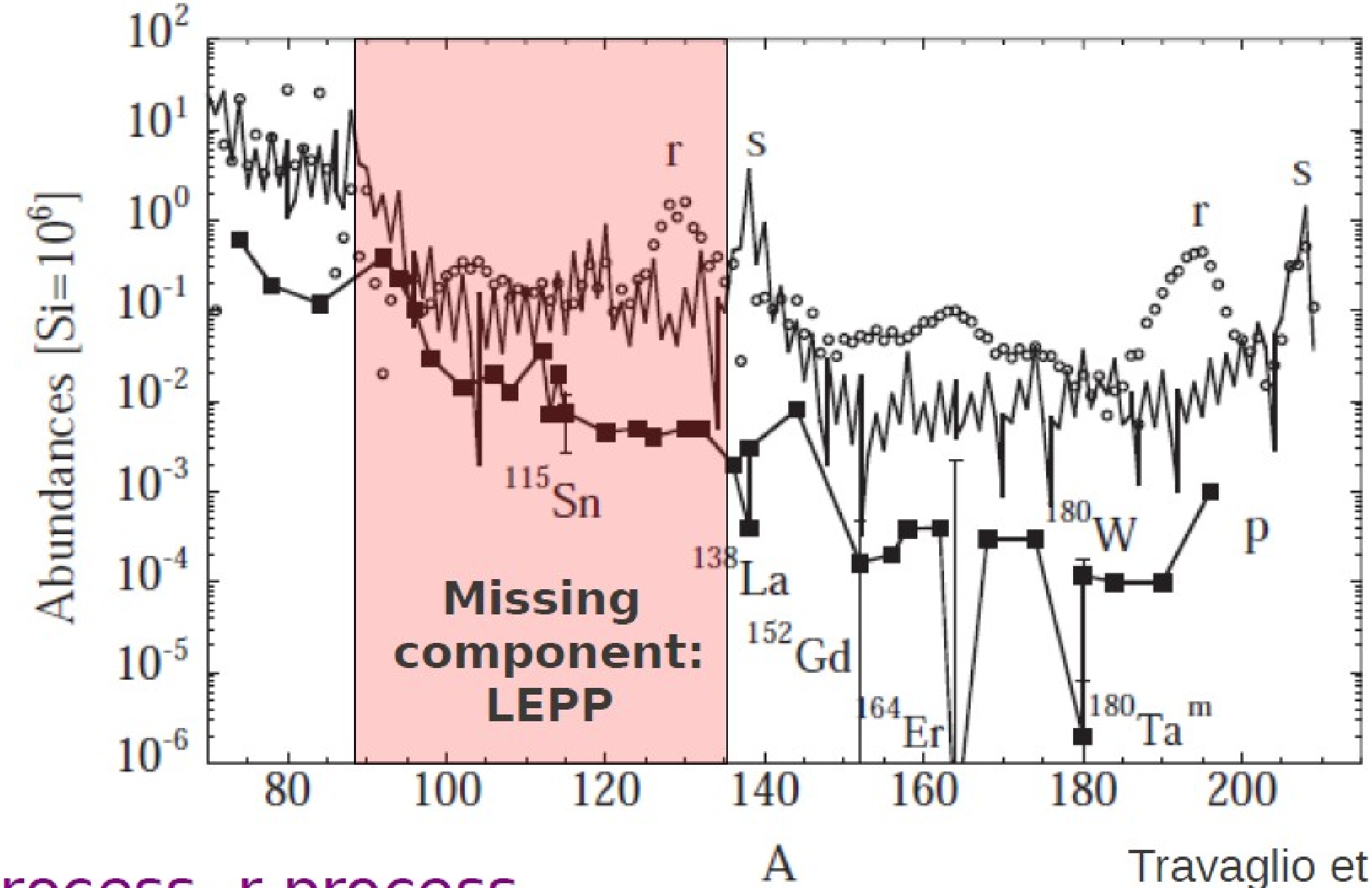

Travaglio et al. 2004

The s-process, r-process and p-process **are not able** to explain all the abundances of the heavy elements above iron (e.g., for silver).

See e.g., Hansen et al. 2012

s-Process Contribution and *r*-Process Fraction at the Solar Composition for Elements from Ru to Cd

Element	*s*-Fraction AGB+weak *s* (%)	*r*-Fraction: *r*-Residuals (%)	*r*-Fraction: From CS 22892−052 (%)
Ru............	24	69	50
Rh............	10	90	43
Pd	36	64	36
Ag............	9	91	30
Cd............	38	62	(41)

- Between the s-process and the r-process in 1977 it was defined the intermediate neutron-capture process.

In 1996 it was observed for the first time an i-process carrier.

i-process ~ 10^{15} n cm^{-3}
Cowan & Rose 1977 ApJ
Herwig, MP et al. 2011 ApJ

Sakurai's object

hs = Ba peak
ls = Sr peak

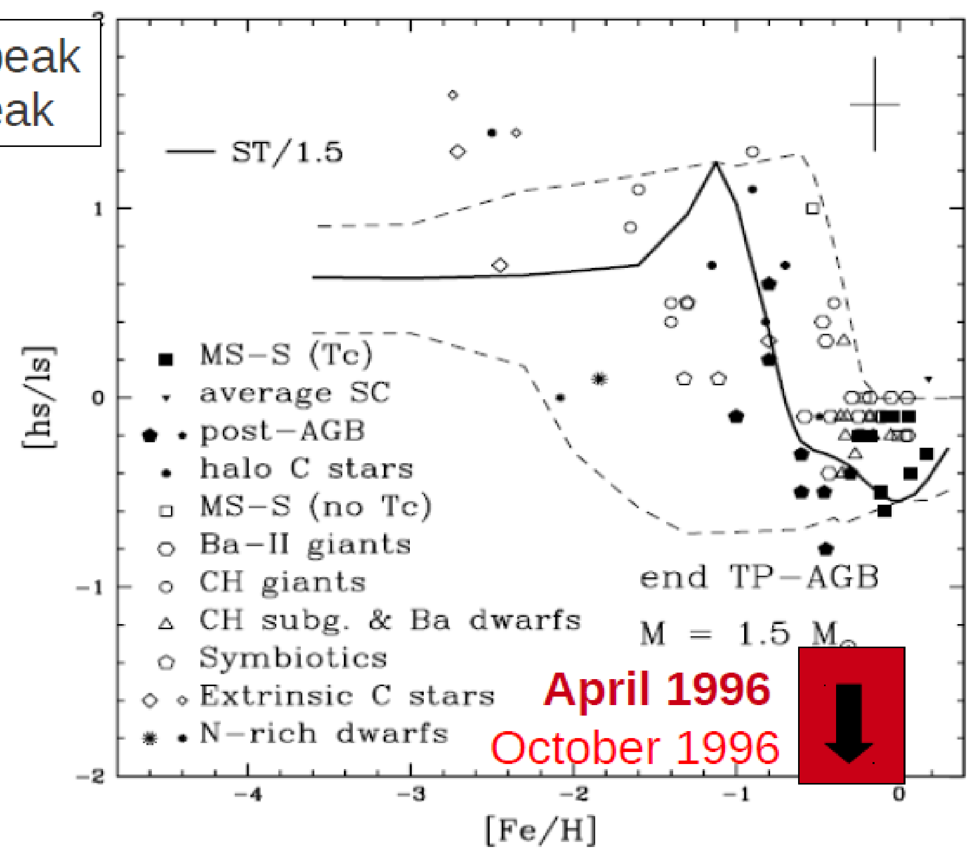

Busso et al. 2001, ApJ 557 versus
Asplund et al. 1999 A&A 343

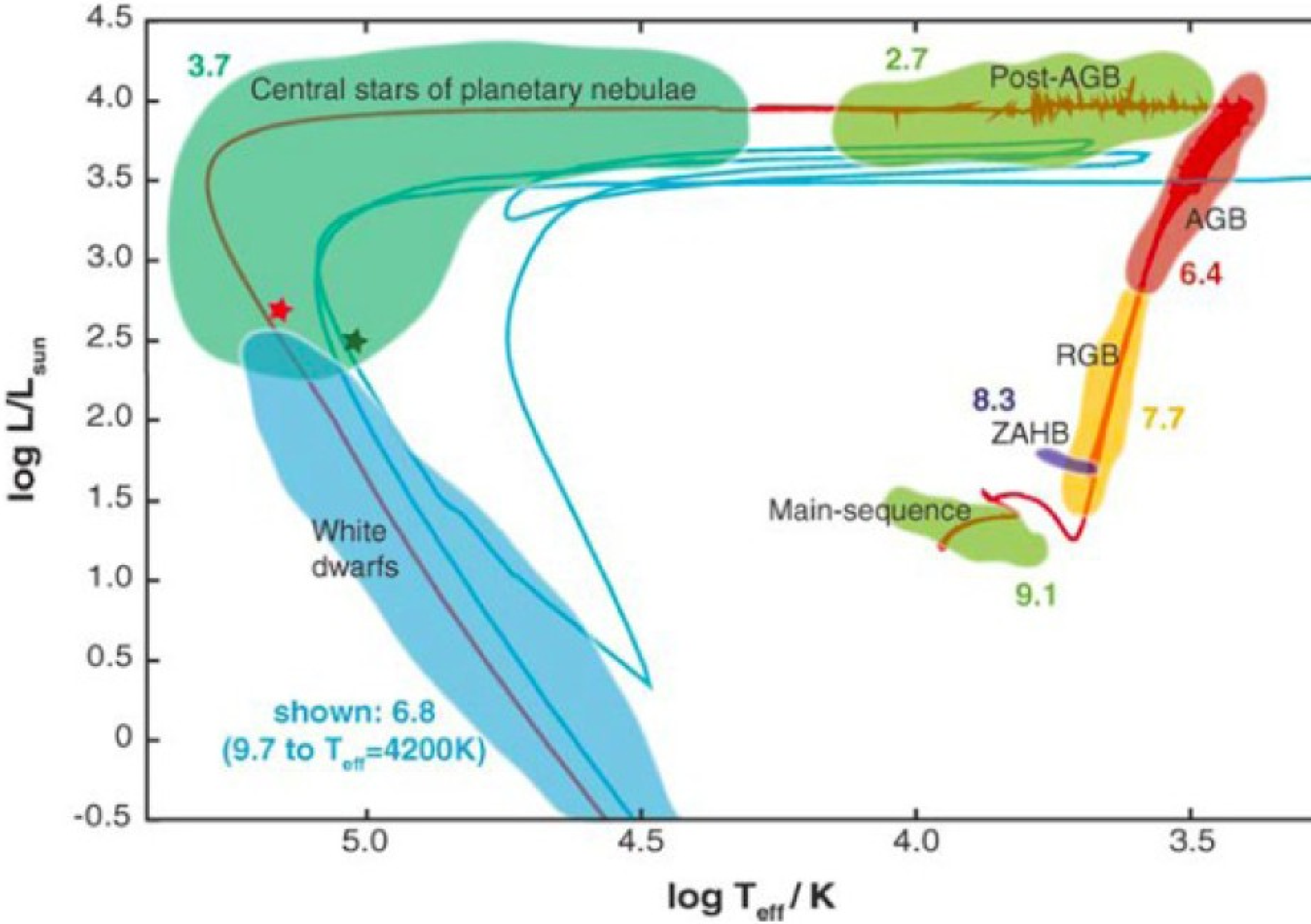

Werner & Herwig 2006, PASP

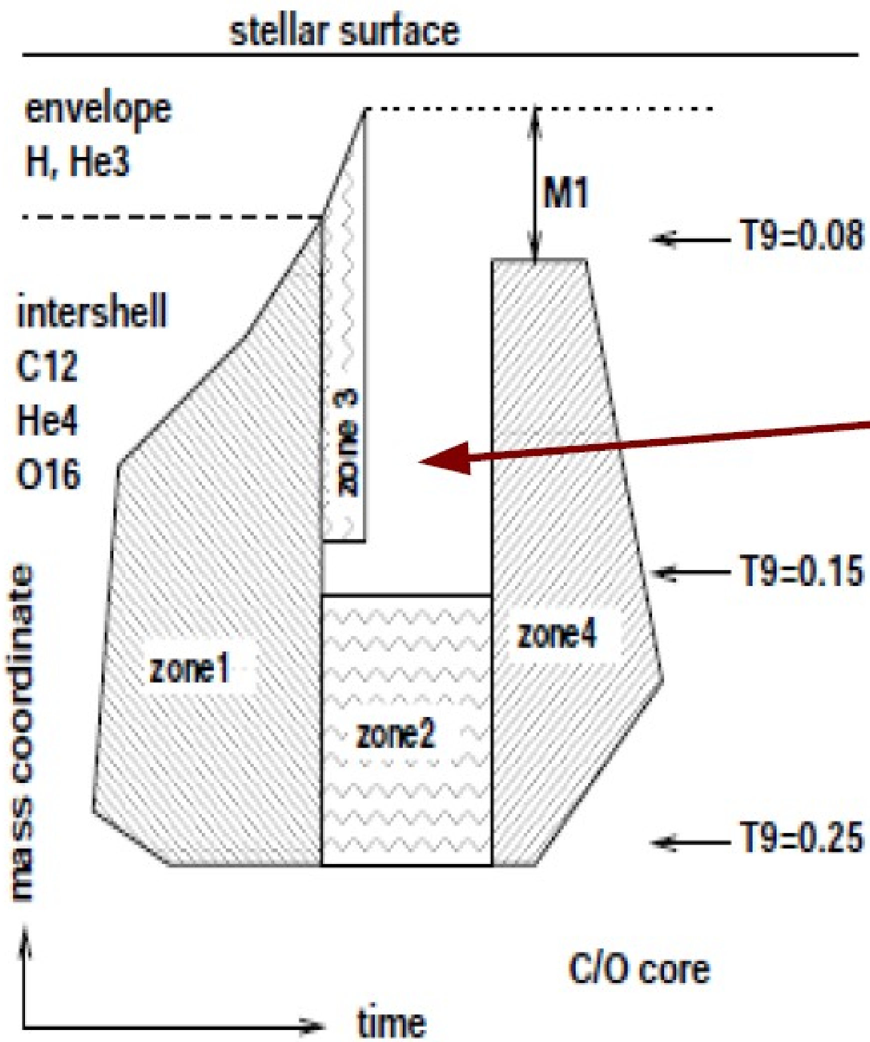

C12+p → N13
N13 → C13

Herwig et al. 2001
astroph 0103004

Figure 1 Schematic (not to scale) of the time-evolution of convection zones in the top 0.01 $M_\odot$ of a post-AGB star of 0.6 $M_\odot$ during a VLTP. All shaded areas indicate convectively unstable zones. The two solid horizontal lines in the upper part of the diagram indicate the stellar surface and the mass coordinate of the envelope-intershell (=core) transition.

hs = Ba peak
ls = Sr peak

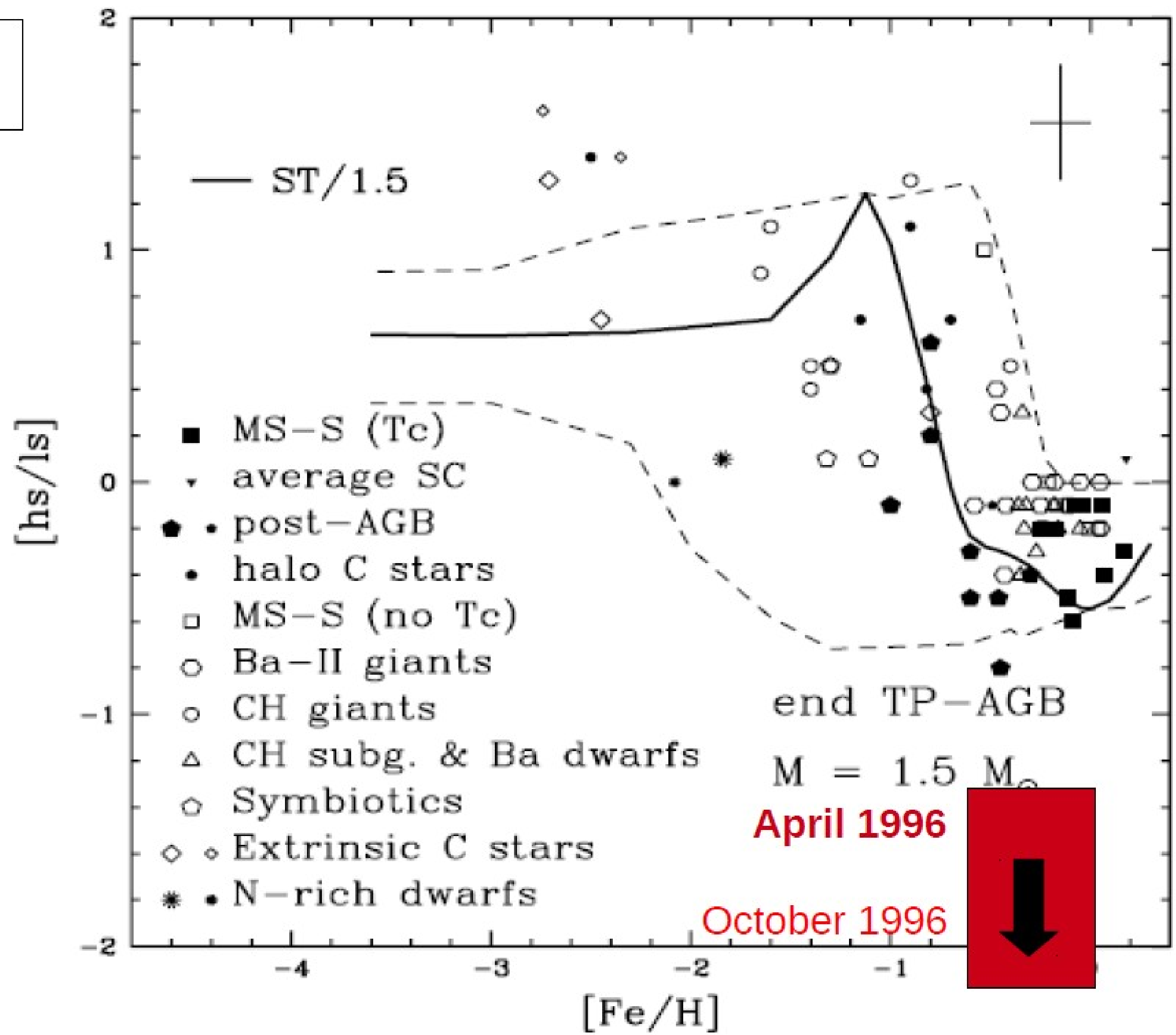

Busso et al. 2001, ApJ 557 versus
Asplund et al. 1999 A&A 343

Multi-zone 1D nucleosynthesis simulations: 3D effects important

Modeling the abundance in post-AGB star Sakurai's object

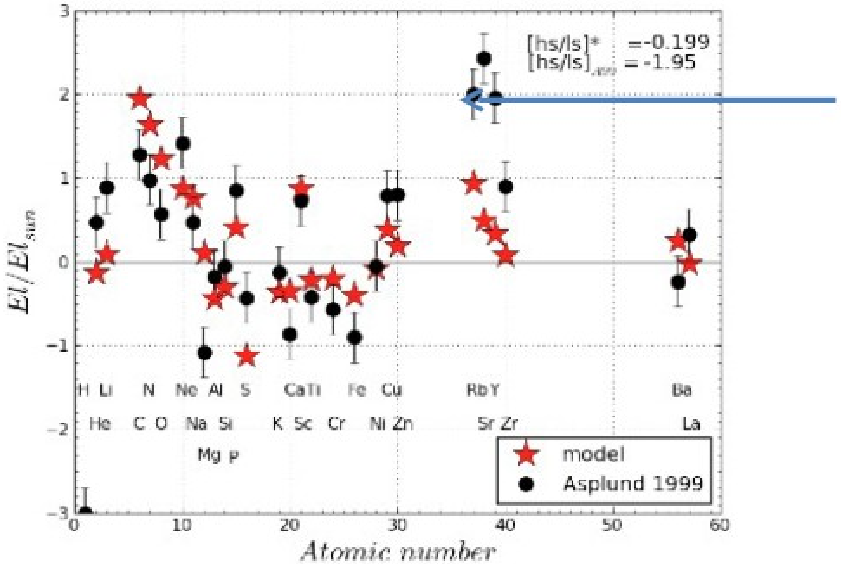

Simulations according to 1D stellar evolution: early thin burning front of 12C + p chokes off mixing

Marginal activation of the C13(α,n)O16, not consistent with the observations.

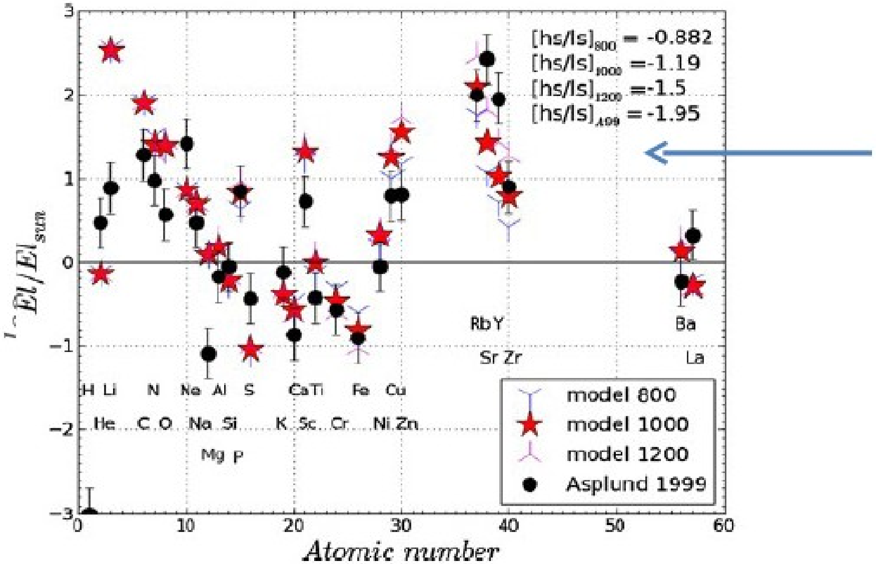

Simulations with extended mixing:
split scenario from 1D simulations does not work. H/N13/C13 reach deeper He-burning layers, activating the i process via the C13(α,n)O16 neutron production.

Herwig, MP et al. 2011, observations: Asplund etal. 1999

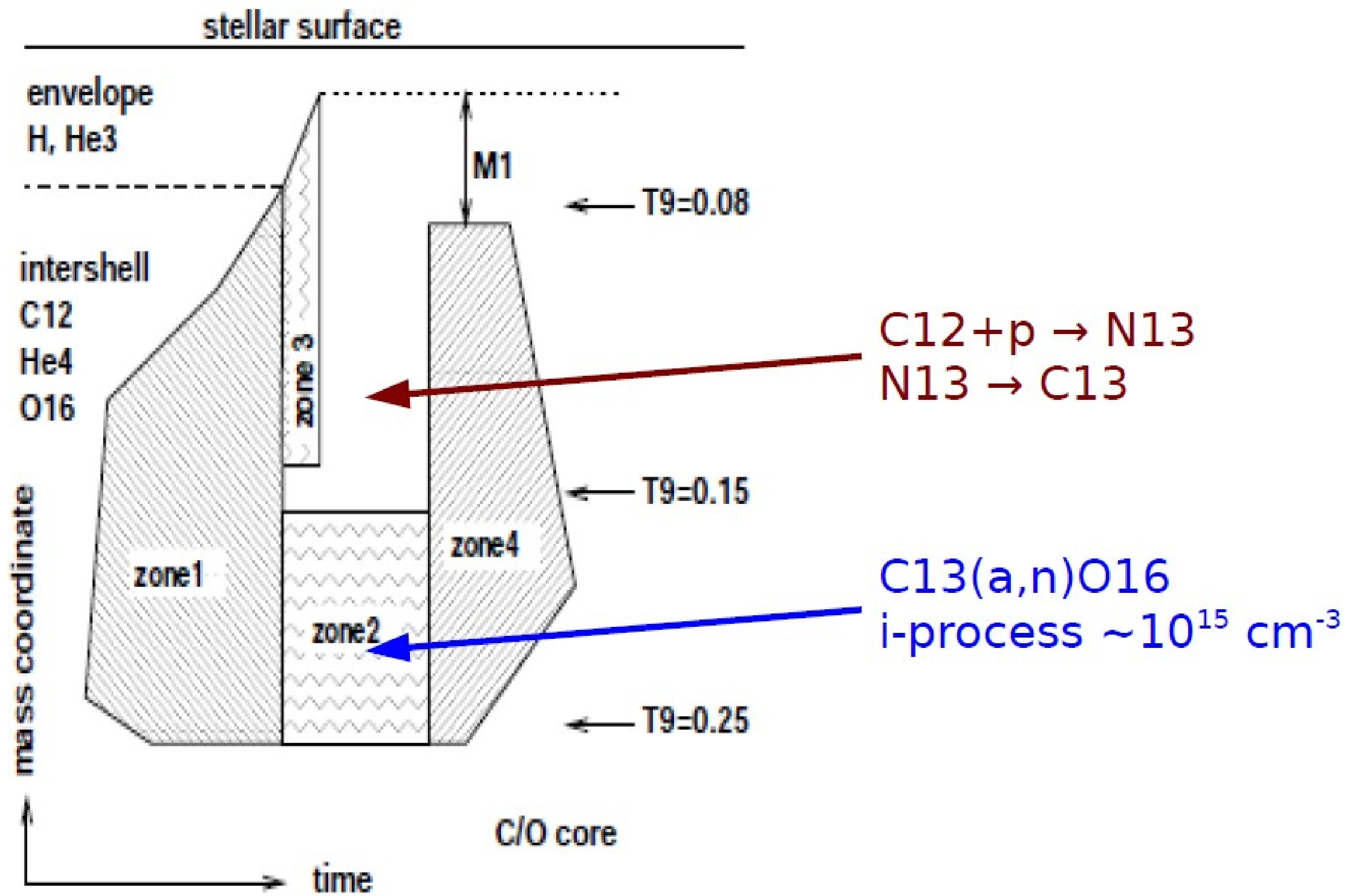

Figure 1 Schematic (not to scale) of the time-evolution of convection zones in the top 0.01 $M_\odot$ of a post-AGB star of 0.6 $M_\odot$ during a VLTP. All shaded areas indicate convectively unstable zones. The two solid horizontal lines in the upper part of the diagram indicate the stellar surface and the mass coordinate of the envelope-intershell (=core) transition.

First scenario:
Delayed split in 3D stellar hydro of H-12C combustion

Stellar hydrodynamics code by **Paul Woodward**, Minnesota.

Formation of split after ≈480min →hydro simulation confirms and agrees with nucleosynthesis analysis prediction of delayed split formation.

grid: 7683
1.47M time steps
0.53M CPU hrs
2056 cores
(ComputeCanada, WestGrid)

Confirmed with 11523 run performed on **NSF Blue Waters** (LCSE, 2.7M CPU hrs).

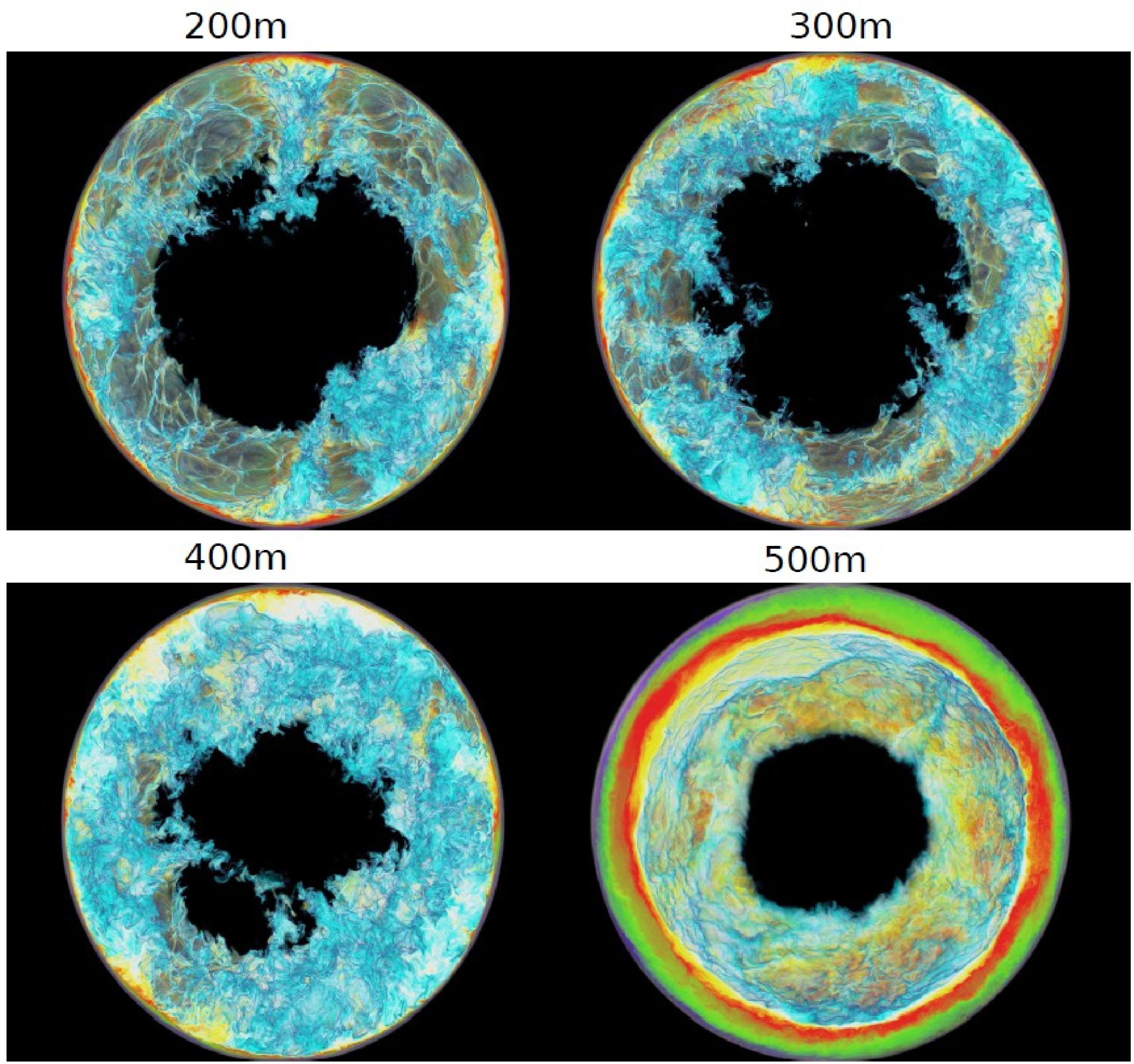

Impact of 12C(p,γ)13N reaction rate on hydrodynamic combustion feedback

- Additional run (right panel) with reaction rate 12C(p,γ)13N * 0.5 performed by **Paul Woodward** and his research team at Minnesota.
- Run on newest NSF supercomputer **Blue Waters: 11.27**, running on 110,656 cores for 11.27hrs

Standard 12C(p,γ)13N   Snapshot at 485m   12C(p,γ)13N * 0.5

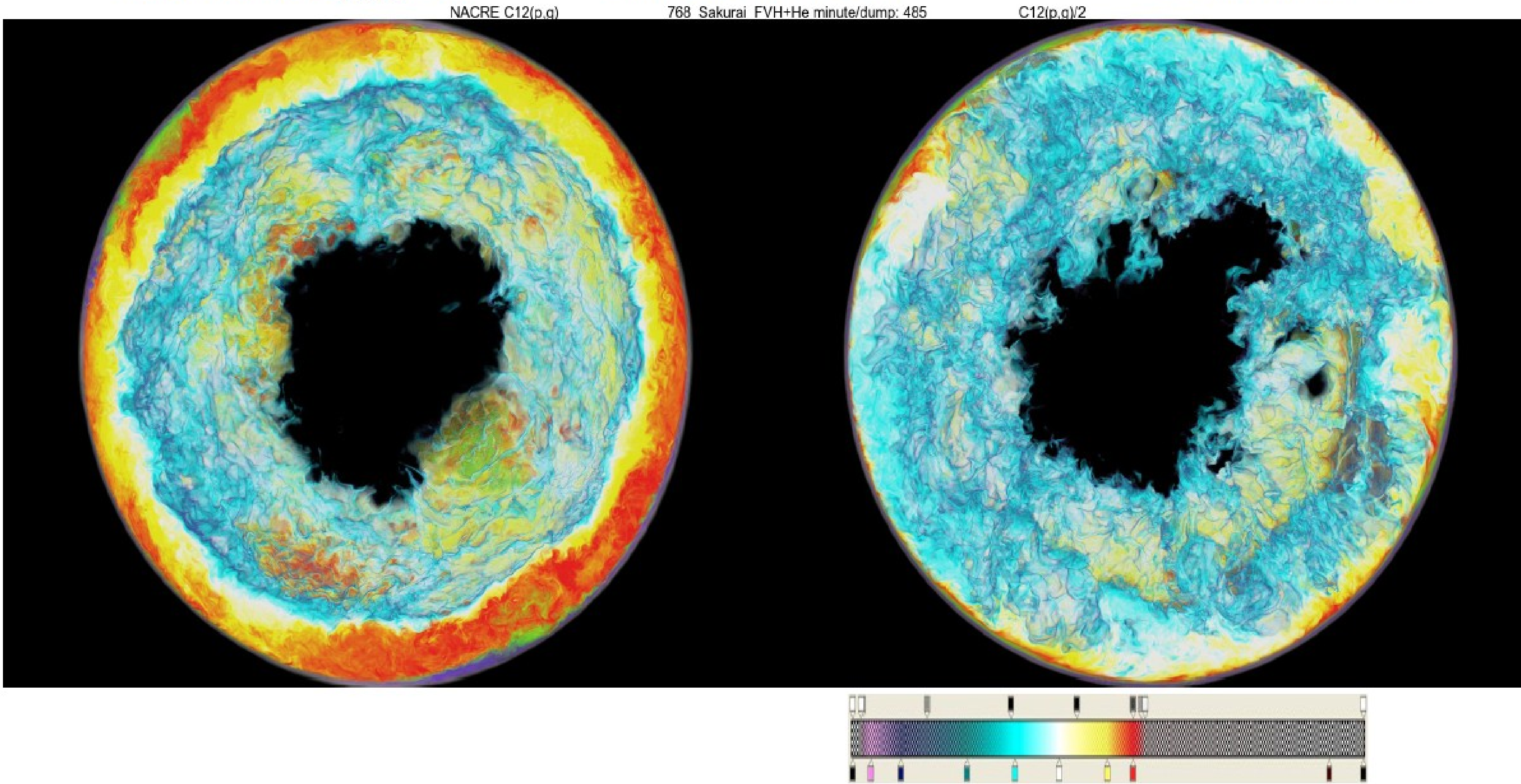

Most recent results for the hydrodynamics of H ingestion:

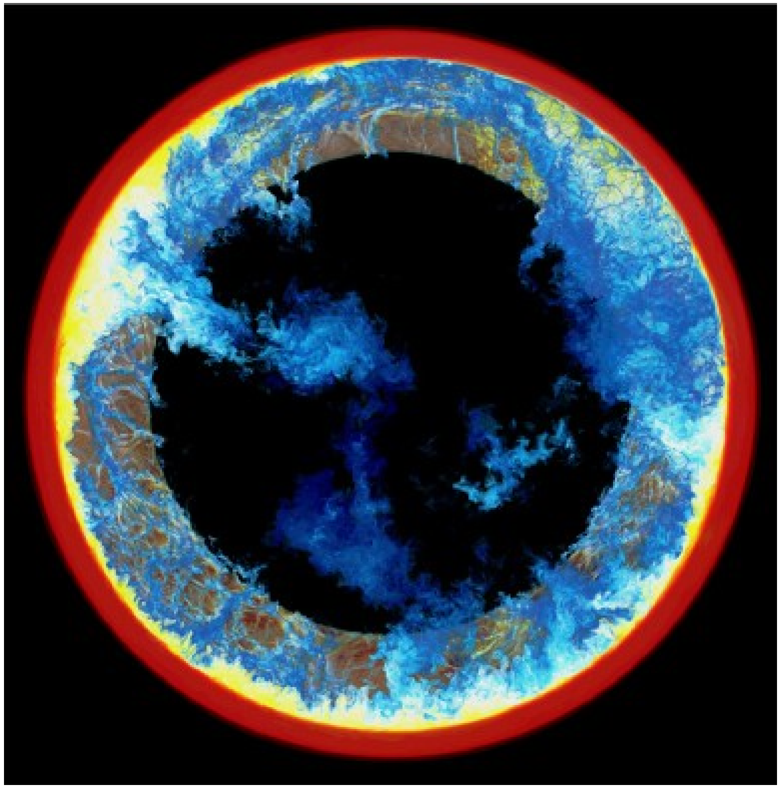

Woodward et al. 2014, arXiv1307.3821
Herwig et al. 2014, arXiv1310.4584

- Analysis of the entrainment process at the top convection boundary and on the subsequent advection of H-rich material into deeper He-rich layers.

- Defined the quantitative dependence of the entrainment rate on grid resolution.

Future step:
include limited network with virtual species and virtual neutron capture rates, to evaluate the neutron density distribution and the neutron exposure.

Nucleosynthesis properties of the i process: Se-Nb

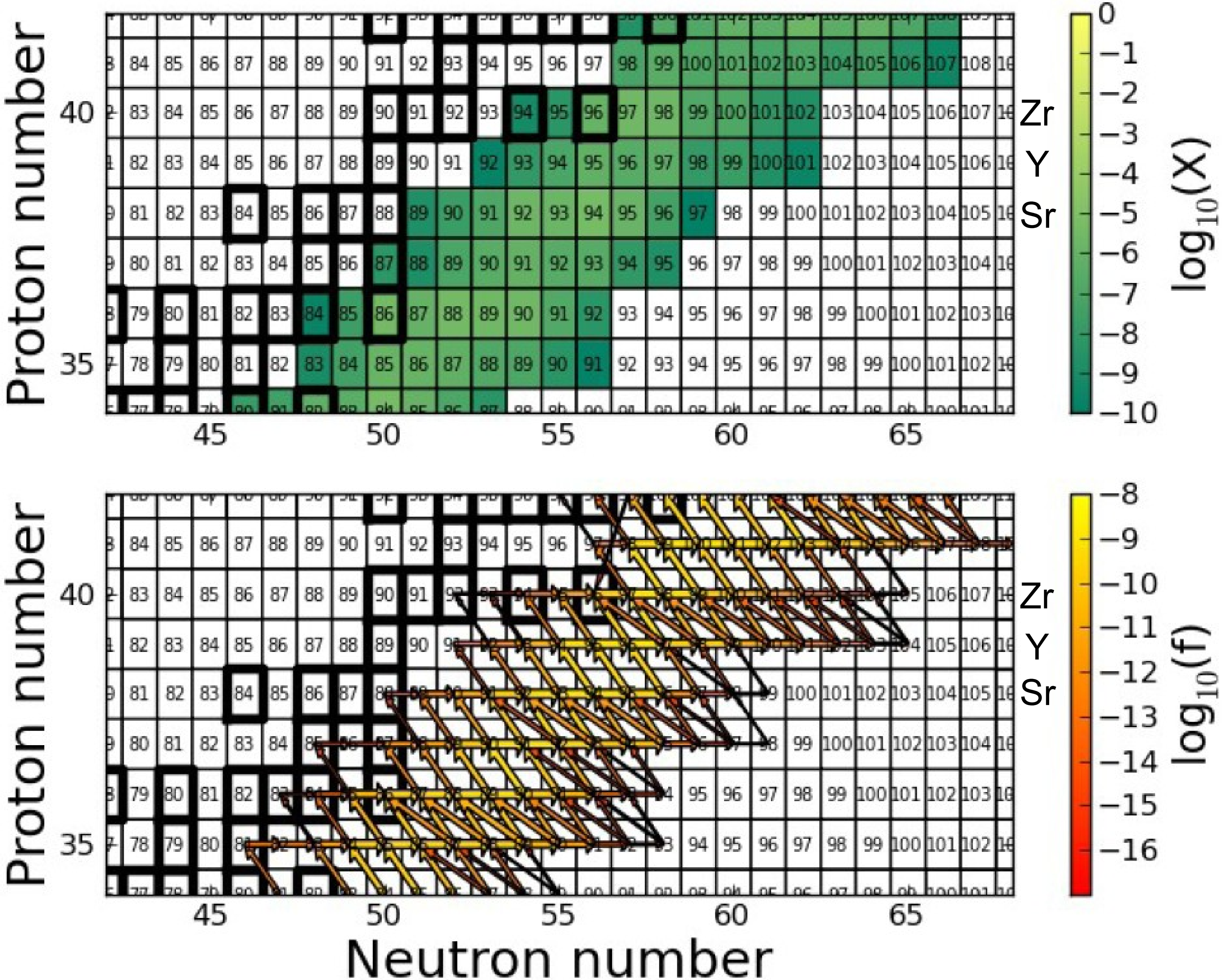

Nucleosynthesis properties of the n process: Se-Nb

(Blake & Schramm 1976)

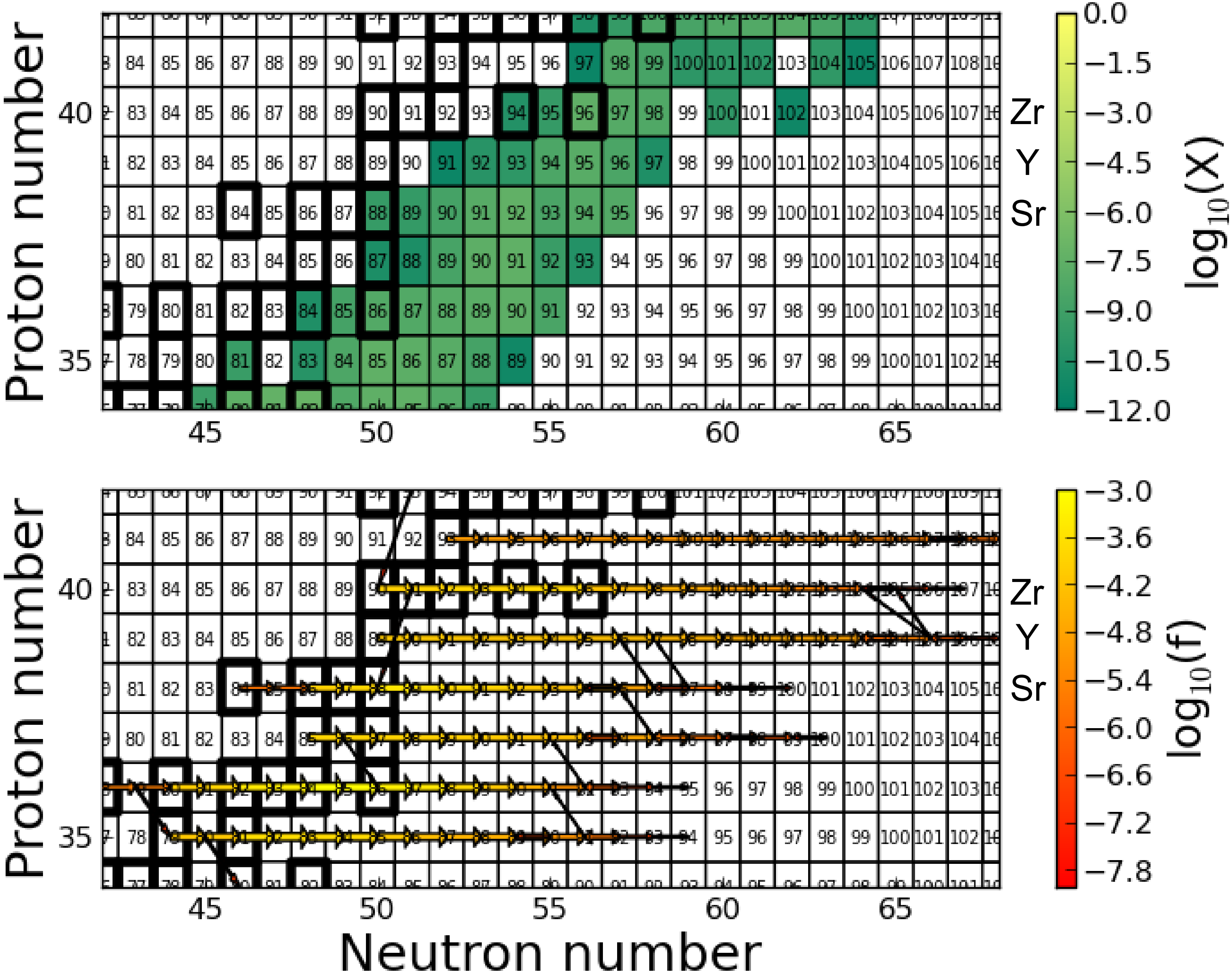

CCSN

Presolar grain from an old CCSN

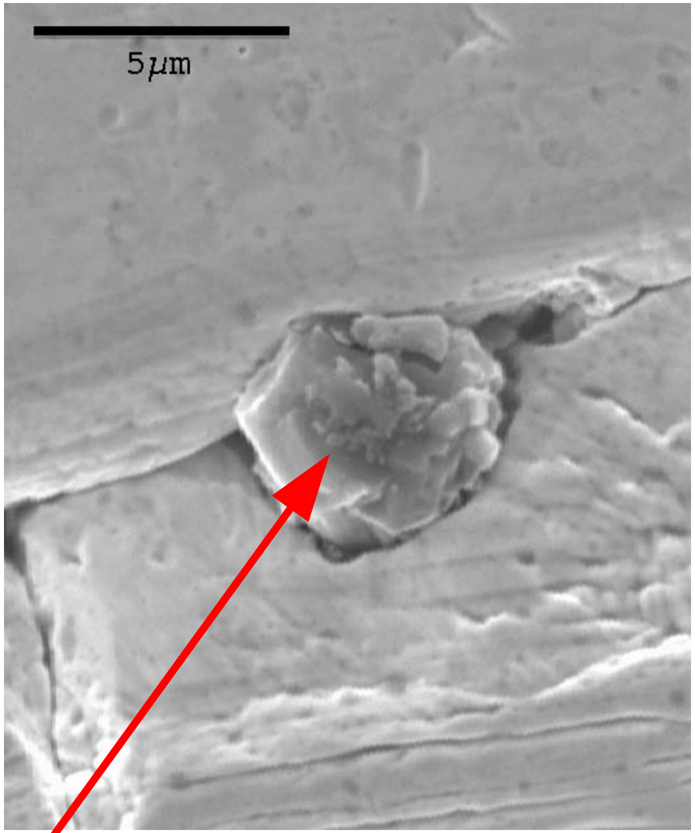

Cas A
11000 ly
~ 300 years ago

unknown
?
~ 4.5-5 Gy ago

n-process signature (...)
on isotopic ratios of
heavy isotopes
(e.g., Zinner 2003)

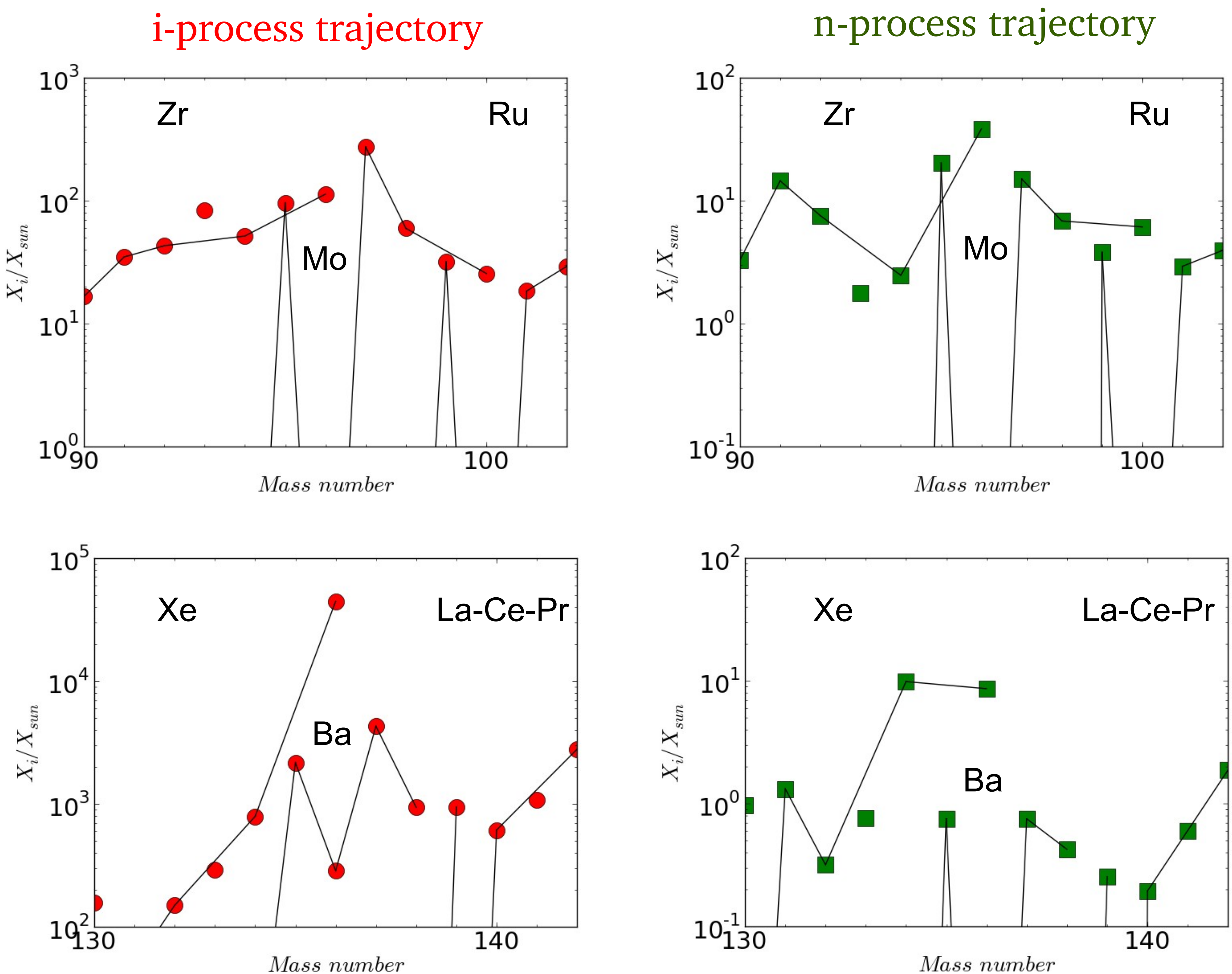
i-process trajectory
n-process trajectory
Zr
Ru
Mo
Zr
Ru
Mo
Xe
La-Ce-Pr
Ba
Xe
La-Ce-Pr
Ba
X_i/X_{sun}
Mass number
90
100
130
140
10^0
10^1
10^2
10^3
10^4
10^5
10^{-1}

Fujiya et al. 2013, ApJL
(SiC AB presolar grains)

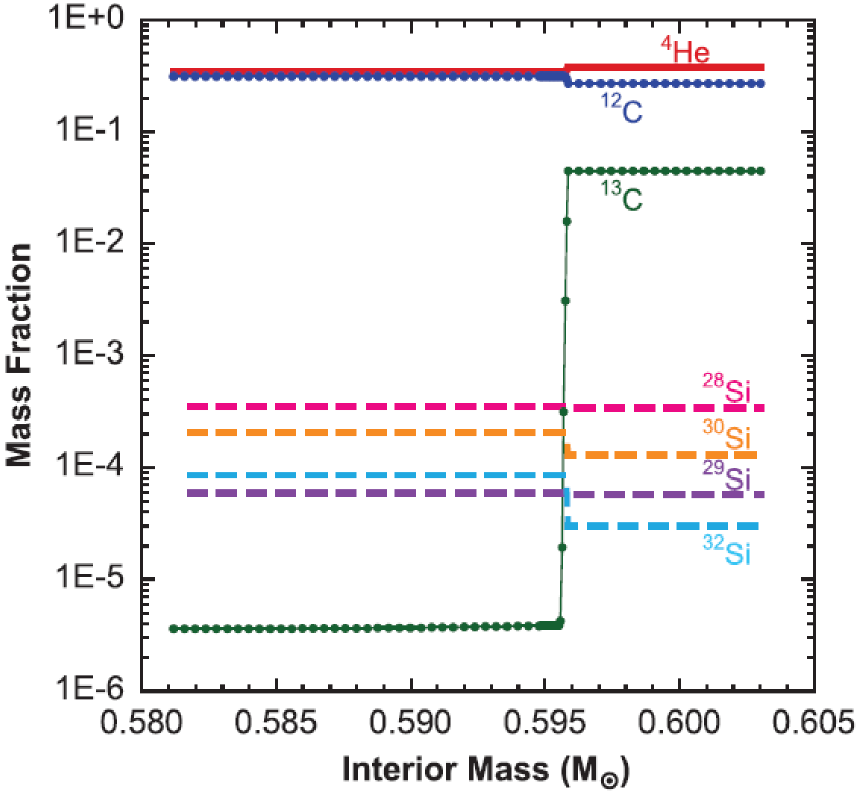

^{31}S 2.57 s β+	^{32}S 95.02 4.1 mb	^{33}S 0.75 7.4 mb	^{34}S 4.21 0.226 mb	^{35}S 87.51 d β-
^{30}P 2.50 m β+	^{31}P 100 1.74 mb	^{32}P 14.26 d β-	^{33}P 25.34 d β-	^{34}P 12.43 s β-
^{29}Si 4.683 7.9 mb	^{30}Si 3.087 6.5 mb	^{31}Si 2.62 h β-	^{32}Si 132.02 a β-	^{33}Si 6.18 s β-
^{28}Al 2.24 m β-	^{29}Al 6.56 m β-	^{30}Al 3.60 s β-	^{31}Al 644.00 ms β-	^{32}Al 33.00 ms β-
^{27}Mg 9.46 m β-	^{28}Mg 20.91 h β-	^{29}Mg 1.30 s β-	^{30}Mg 335.00 ms β-	^{31}Mg 230.00 ms β-

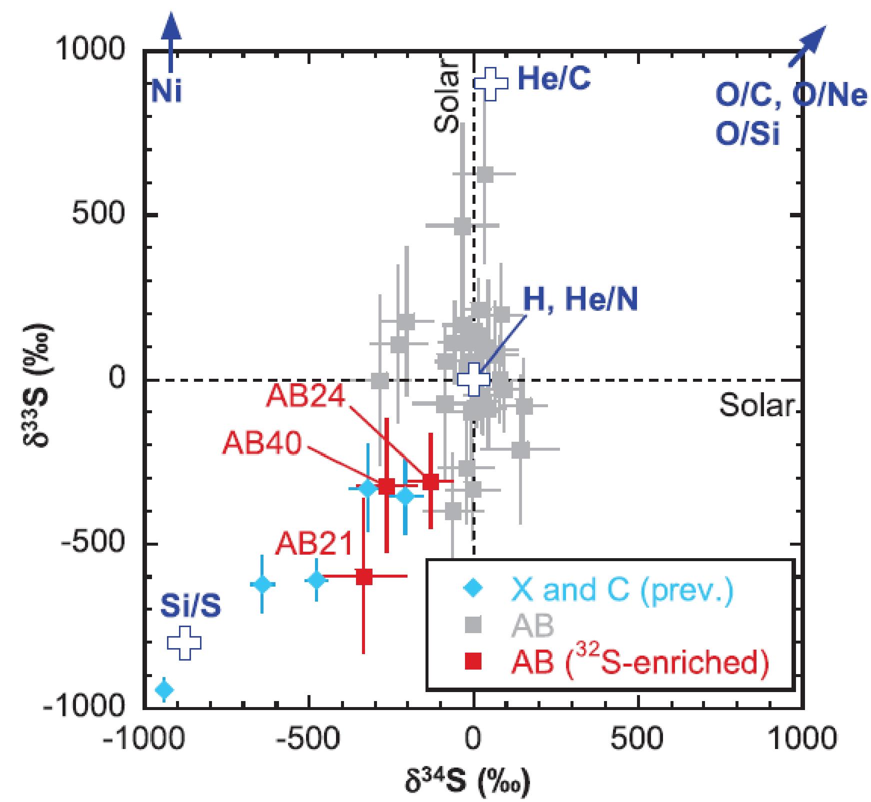

Liu et al. 2014, ApJ accepted (Mainstream SiC grains)

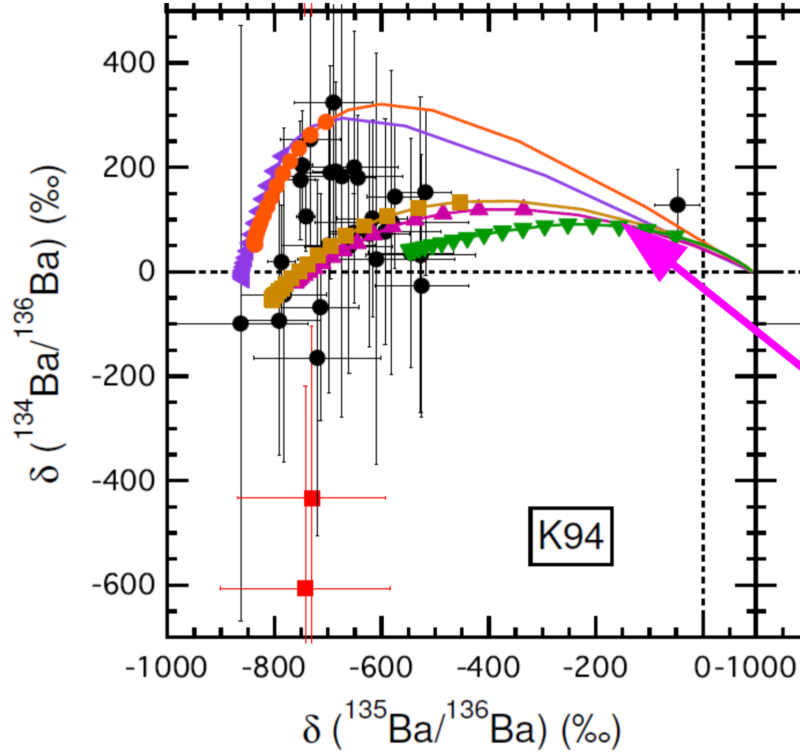

Roberto's AGB models

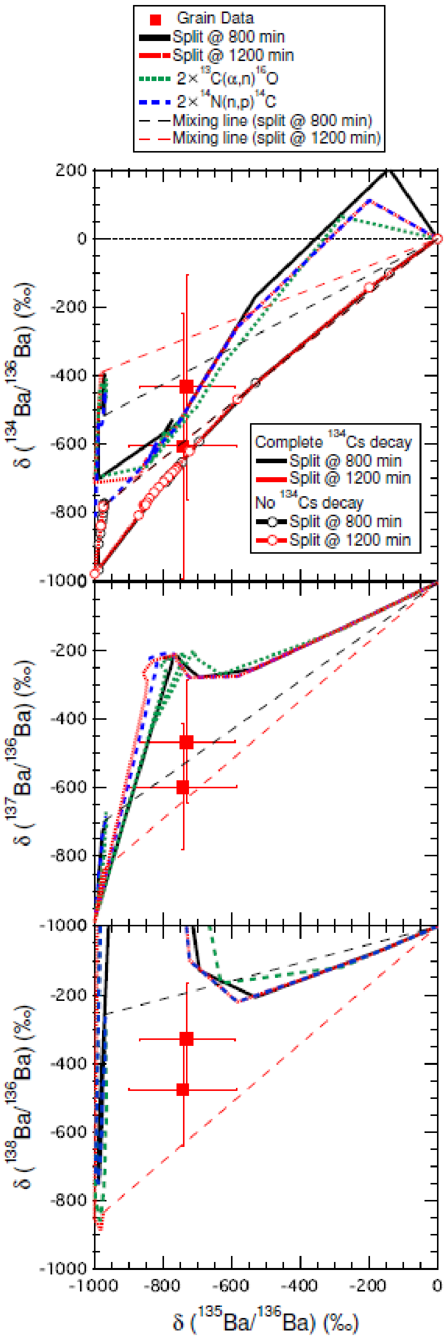

Comparison with FH, MP et al. 2011

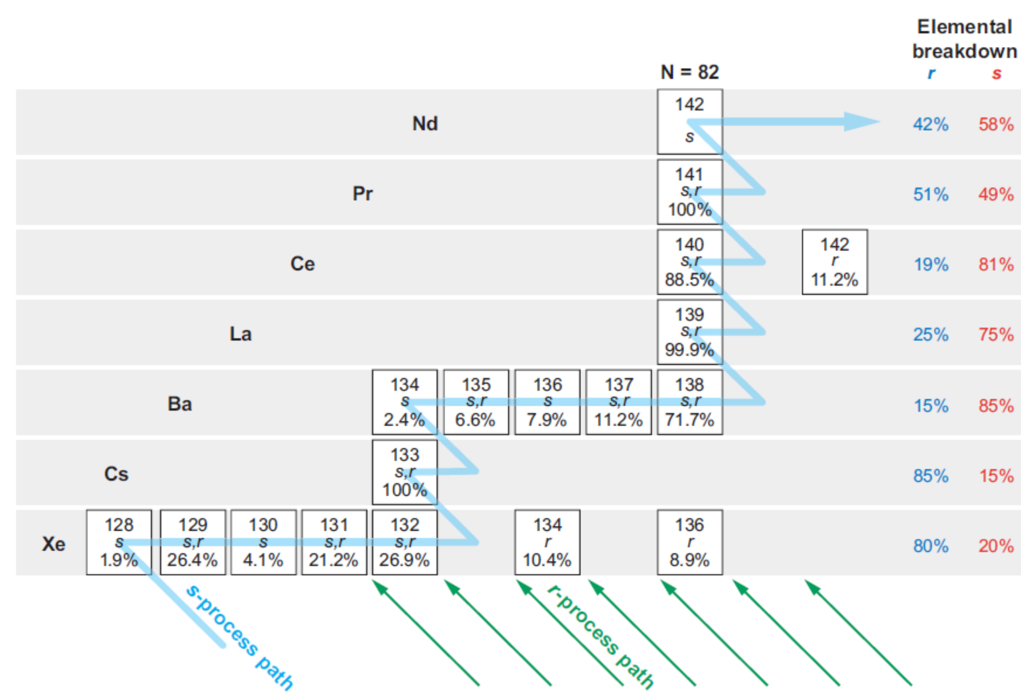

Observations over a large sample of OH/IR stars in our Galaxy, LMC and SMC extreme enrichment of Rb and high Rb/Zr in massive AGB stars (4-8 Msun).

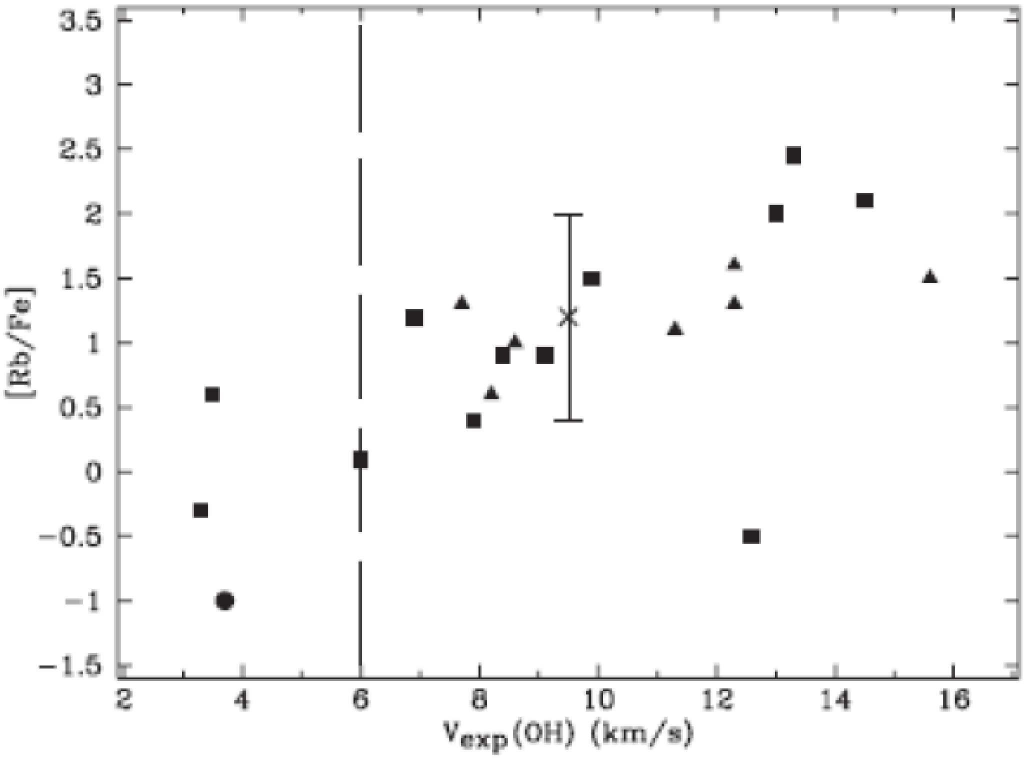

Garcia-Hernandez et al. 2006,
Garcia-Hernandez et al. 2009

Karakas et al. 2012

The s process cannot produce a large Rb/Zr ratio

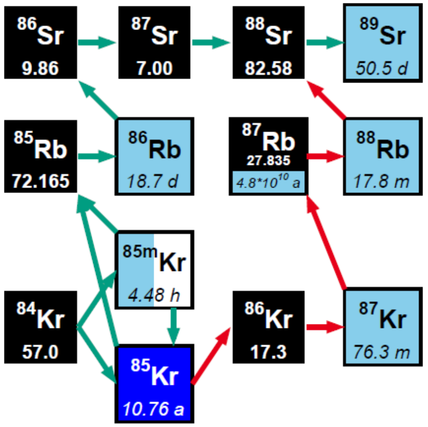

Problem for GCE

CEMP-rs stars → CEMP-i stars

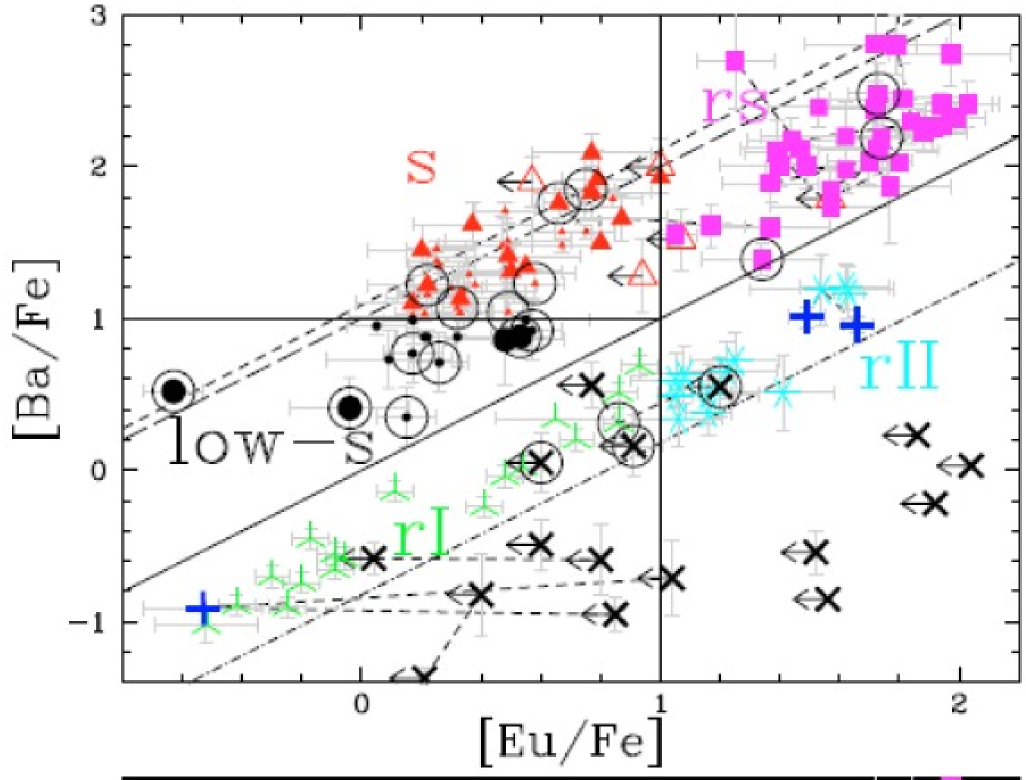

Masseron et al. 2010

~ 20% of the low metallicity stars are carbon-rich (Lucatello et al. 2006)

Bertolli, MP et al. 2013, arXiv
Herwig, MP et al. 2014, in prep.

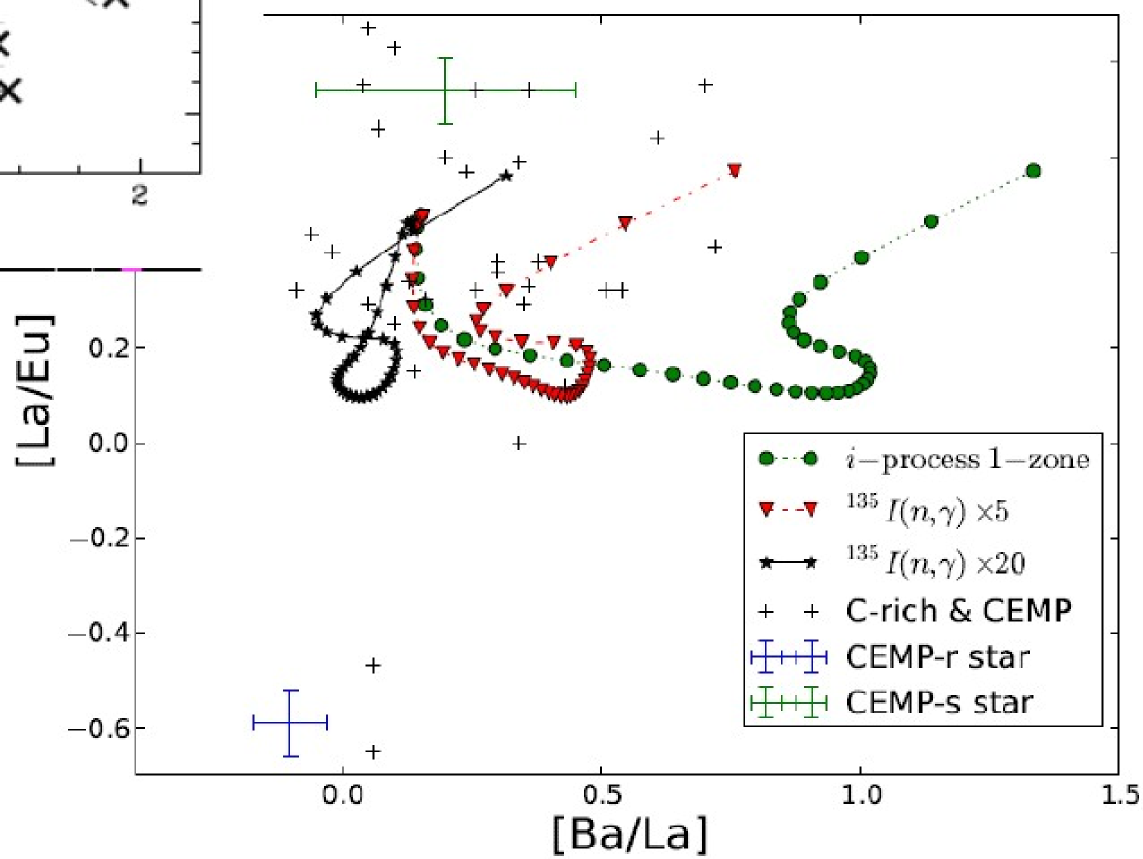

What is the Origin of the Elements?

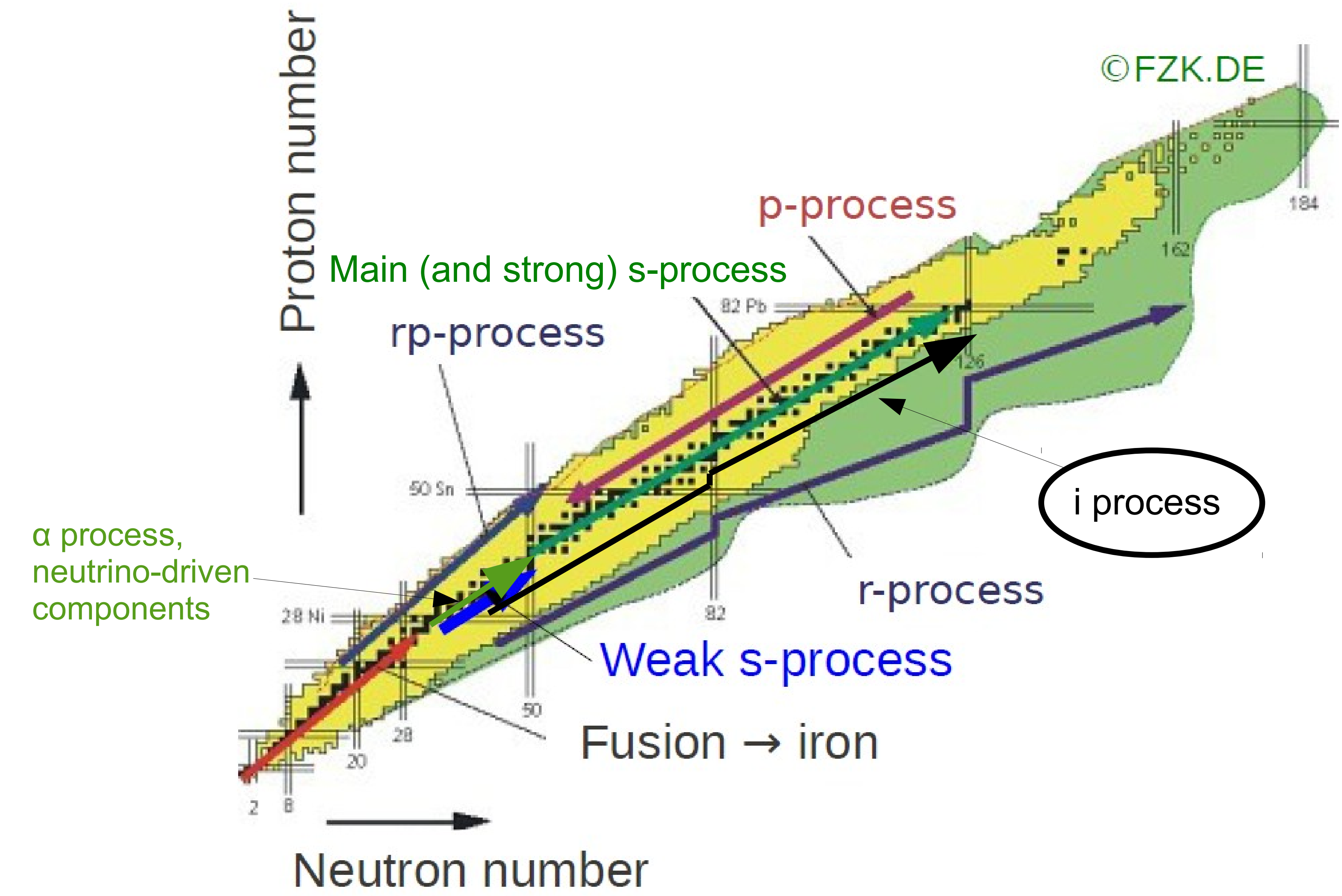

www.nugridstars.org

NuGrid stats:

15 institutions
16 senior investigators
25 post-docs and students

Acknowledgements:

NuGrid acknowledges significant support from NSF grants PHY 02-16783 and PHY 09-22648 (Joint Institute for Nuclear Astrophysics, JINA) and EU MIRG-CT-2006-046520. The continued work on codes and in disseminating data is made possible through funding from STFC (RH, UK), an NSERC Discovery grant (FH, Canada), and an AMBIZIONE grant of the SNSF (MP, Switzerland). NuGrid computations are performed at the Arizona State University's Fulton High-performance Computing Center (USA), the high-performance computer KHAOS at EPSAM Institute at Keele University (UK) as well as CFI (Canada) funded computing resources at the Department of Physics and Astronomy at the University of Victoria and through Computing Time Resource Allocation through the Compute Canada WestGrid consortium.